

# Morphology, Order, Light Transmittance, and Water Vapor Permeability of Aluminum-Coated Polypropylene Zeolite Composite Films

Devrim Balköse,<sup>1</sup> Kaan Oguz,<sup>2\*</sup> Lutfi Ozyuzer,<sup>2</sup> Suleyman Tari,<sup>2</sup> Esen Arkis,<sup>1</sup> Filiz Ozmihçi Omurlu<sup>1</sup>

<sup>1</sup>Department of Chemical Engineering, Izmir Institute of Technology, Urla-35430 Izmir, Turkey

<sup>2</sup>Department of Physics, Izmir Institute of Technology, Urla-35430 Izmir, Turkey

Received 9 October 2009; accepted 26 August 2010

DOI 10.1002/app.33300

Published online 1 December 2010 in Wiley Online Library (wileyonlinelibrary.com).

**ABSTRACT:** In this study, the polypropylene-zeolite composite films having 2–6 wt % natural zeolite were coated with a thin film of aluminum (Al) by magnetron sputtering, and the contribution of the Al coating on film properties was investigated. The samples were characterized by EDX, X-ray diffraction, SEM, AFM, UV-visible spectroscopy, and water vapor permeation analyses. The surface of the films coated with a smooth Al film having 98–131 nm thickness. EDX revealed that Al percentage on the surface appeared to be as 8–10 wt % indicating contribution of polymer surface under Al film

to analysis. XRD analysis showed that the grain size of Al at the surface was 22–29 nm. The surface roughness increased after Al-coating process. The transmission of coated films was very low for both UV and visible regions of the light spectrum. Permeation analysis indicated that water vapor permeation was lower for Al-coated material. © 2010 Wiley Periodicals, Inc. *J Appl Polym Sci* 120: 1671–1678, 2011

**Key words:** poly(propylene); aluminum thin films; coatings; zeolites; magnetron sputtering

## INTRODUCTION

Microelectronics industry, flat plate displays, touch screens, IR reflectors, solar cells and optical sensors, pharmaceutical products, catalysts, ceramics, spacecraft, and biomedical applications demand coating of metals onto polymer surfaces. Polymer metallization occur through nucleation, continuous film production, and interface formation steps. To increase the adhesion between metallic film and the polymer, polymer surfaces are modified by plasma techniques. Using oxygen and argon gas,<sup>1,2</sup> corona discharge,<sup>3,4</sup> low-pressure plasma<sup>5,6</sup> are the ways of interfacial enhancement. Interfacial bond play an important role in the enhancement of metal polymer adhesion.<sup>7</sup> Covalent oxygen bonds were responsible for adhesion of aluminum (Al) oxide to polymer surface.

Different polymers such as Capton, Mylar, polypropylene, and polyethylene were ion implanted,<sup>8</sup> and polyethylene and polycarbonate were coated with Al.<sup>9,10</sup> Au, Ag, Pd, Cu, and Ni were coated on

poly(methylmetacrylate) (PMMA) particles by barrel sputtering,<sup>11</sup> and crystalline metallic films were formed on the polymer surface. Ultrathin Al films were deposited on polyethylene terephthalate (PET) by electron ion beam deposition and coatings had grain size in the range of 19.8 and 35.7 nm. Annealing of discontinuous Al film on PET at temperatures close to glass transition temperature of PET resulted in a transient nanocomposite layer having high resistivity and low-light transmittance.<sup>12</sup> Mirrors made by coating of Al alloys on PET had higher photo thermal stability when a thin Ti layer was coated under Al alloys due to grain size and crystalline orientation effects.<sup>13</sup> Al coating obtained by roll-to-roll coating on polypropylene was polycrystalline with grain size 20–70 nm.<sup>14</sup>

Metal-coated polymer films are used in packaging industry for storage of foods in humid atmosphere. For example, Al-laminated polyethylene was used for storing jackfruit powder at relative humidity less than 75 wt % at 25°C.<sup>9</sup>

Gas barrier properties of metal, nonmetal, or metal oxide-coated films are affected by the cracks formed on the coatings.<sup>15</sup> Ti-coated track-etched Lexan polycarbonate and PET membranes could be used for purification of hydrogen gas from carbon dioxide due to higher permeability to hydrogen.<sup>16</sup> Diamond like carbon (DLC)-coated PET, PE, and PMMA membranes had lower oxygen transmission rates

\*Present address: CRANN and School of Physics, Trinity College, Dublin, 2 IRELAND..

Correspondence to: D. Balköse (devrimbalkose@iyte.edu.tr).

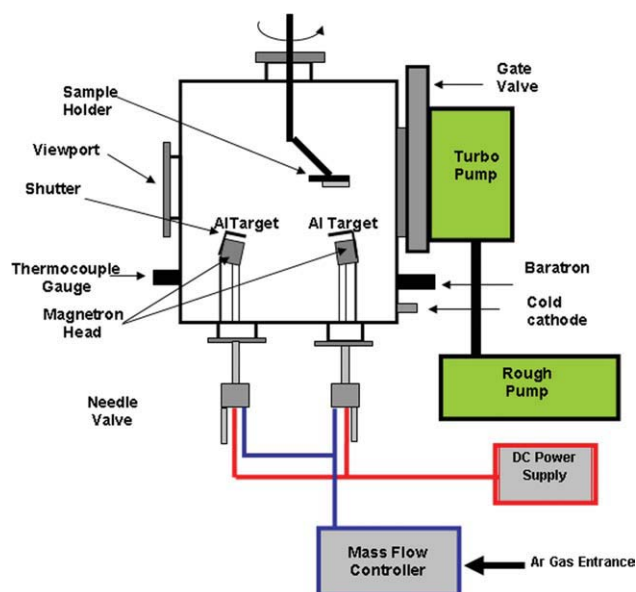


**Figure 1** Magnetron sputtering system. [Color figure can be viewed in the online issue, which is available at [wileyonlinelibrary.com](http://wileyonlinelibrary.com).]

than uncoated films. The higher the residual strain of DLC-coated films upon release of tensile stress, the higher was the oxygen transmission rate.<sup>17</sup> Sorp-

tion behavior of water and water vapor was investigated by Ozmiş et al.,<sup>18</sup> on polypropylene zeolite composites, and the effect of 2–6 wt % zeolite contributed water sorption to the polypropylene. Films with zeolite adsorbing moisture up to 0.5 wt % and being permeable to water vapor could be used as a desiccating packing material if their external surface was coated with a barrier film. For this purpose, polypropylene zeolite composite was coated with Al, and contribution of Al coating on desiccating packaging material behavior was investigated in this study. The objective of the study is to have a packing material that is impermeable to light, impermeable to moisture from outer surface, and permeable to water and adsorbing moisture from inner surface.

## MATERIALS AND METHODS

### Materials

Polypropylene pellets (Petkim MH418 PP) with a density of  $0.89 \text{ g cm}^{-3}$  and an isotactic index of 0.75 were used in the experiments. Natural zeolite from Gördes Manisa having composition 10 wt %  $\text{Al}_2\text{O}_3$ , 0.1 wt % BaO, 1.5 wt % CaO, 0.6 wt % FeO, 1.4 wt %  $\text{K}_2\text{O}$ , 0.9 wt % MgO, 0.3 wt %  $\text{Na}_2$ , 77.5 wt %  $\text{SiO}_2$ , and 22 wt %  $\text{H}_2\text{O}$  was ground by ball mill,

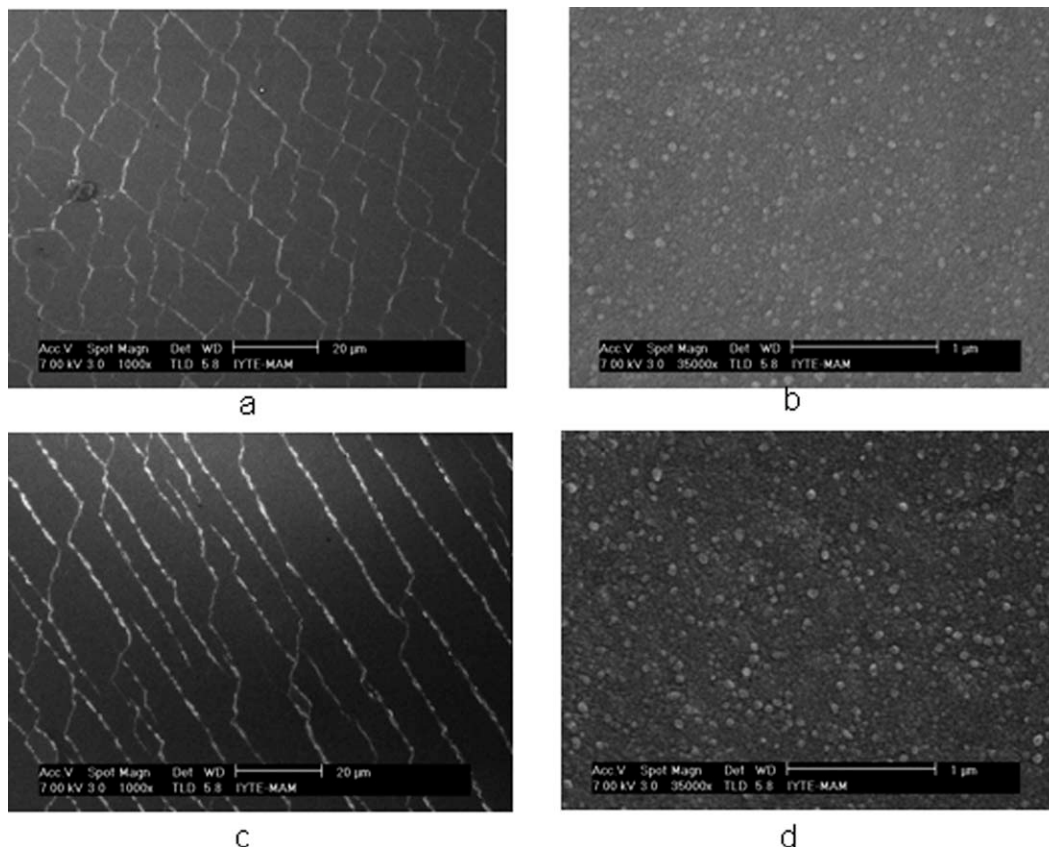


**Figure 2** SEM microphotographs of top of the Al-coated films. (a) PP film 1000 $\times$  magnification, (b) PP film 35,000 $\times$  magnification, (c) 2 wt % zeolite-pp film 1000 $\times$  magnification, (d) 2 wt % zeolite-pp film 35,000 $\times$  magnification.

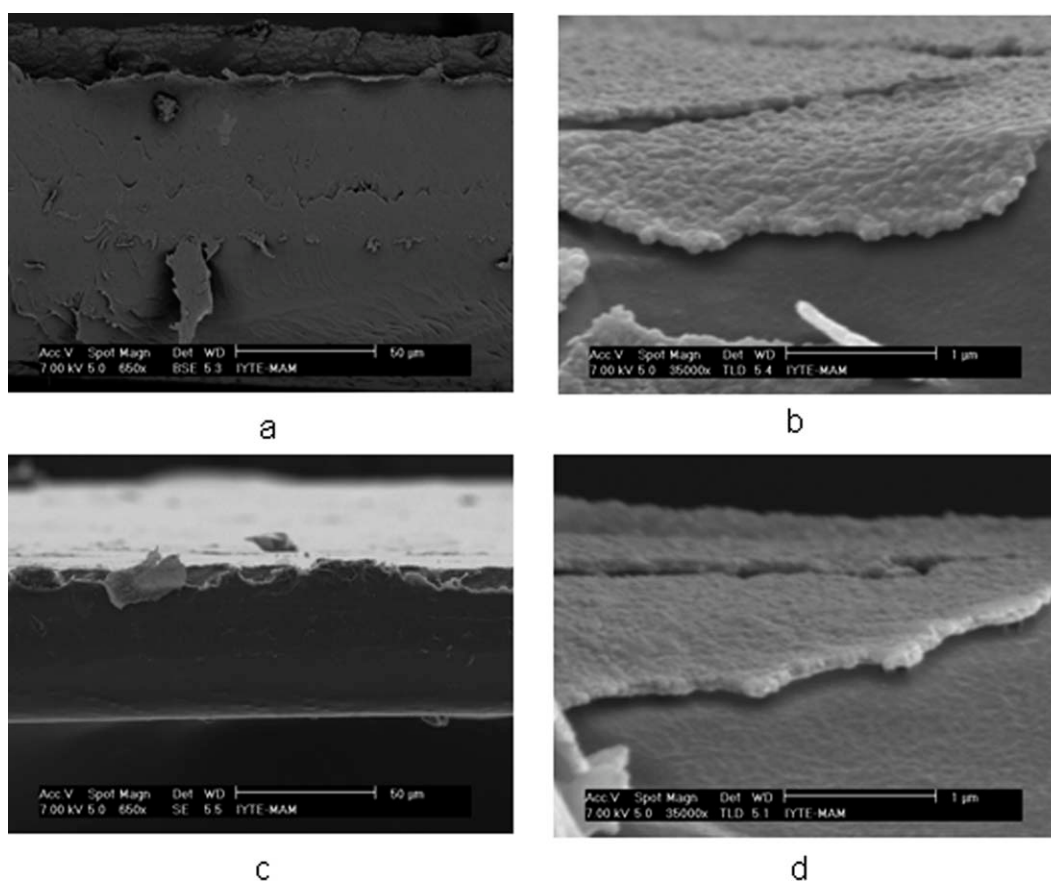


**Figure 3** SEM microphotographs of the cross sections of the Al-coated films. (a) PP film 650 $\times$  magnification, (b) PP film 35,000 $\times$  magnification, (c) 2 wt % zeolite-pp film 650 $\times$  magnification, (d) 2 wt % zeolite-pp film 35,000 $\times$  magnification.

and 2- $\mu\text{m}$  particle size fraction was used in composite preparation.

### Methods

Polypropylene films with 0, 2, 4, and 6 wt % zeolite having 50  $\mu\text{m}$  thickness were prepared by Ozmiççi et al.<sup>18</sup> using a Tonable Plastic single screw extruder. The yield stress values of the films were 35, 26, and 27  $\text{N}/\text{mm}^2$ , and their elongation at break values were 164, 204, and 205%, respectively, for the zeolite filler content of 0, 2, and 4 wt %, respectively. The crystallinity of the films was 30, 38, 42, and 35% as determined by differential scanning calorimetry from films with 0, 2, 4, and 6% zeolite-filled films, respectively. Zeolite filler made the films adsorb water vapor up to 0.5 wt % and permeable to water vapor.<sup>18</sup>

The Al films on polypropylene were deposited by the high-vacuum magnetron sputtering system having four sputtering guns as shown in Figure 1. The base pressure of the system was kept below  $2.6 \times 10^{-4}$  Pa, using a turbo molecular pump. To create the plasma, Ar gas was used (99.99 wt %). The deposition pressure was around 0.65 Pa, and the Ar gas

flow was 0.66  $\text{cm}^3/\text{s}$  under standard temperature and pressure as controlled by a MKS gas flow controller and a baratron gauge. The polypropylene films fixed on glass substrates were coated by condensation of Al atoms sputtered from the target. In the sputtering process, 20-W dc power and 20 mA current were applied to pure Al target.

Morphology of the samples was determined by scanning electron microscopy (Phillips XL-305 FEG-SEM). Elemental composition of the samples was determined by using energy dispersive X-ray spectroscopy (Phillips XL-305 FEG-SEM). The surface of the films was also examined by atomic force microscopy (Nanoscope IV from Digital Instruments). The surface roughness of the samples was determined by the instrument using "Roughness" procedure of standard software. This procedure calculates the root mean square of the scattering of the height values in the height image acquired on the surface. The crystal structure of samples was analyzed by X-ray diffraction (Phillips Phillips X'Pert Pro) using  $\text{Cu K}\alpha$  radiation. Light transmittance was determined by using PerkinElmer UV-vis spectrophotometer. Water vapor permeability was measured by using permeation test apparatus reported previously.<sup>19</sup>

## RESULTS AND DISCUSSION

A negative voltage of  $-1000$  V is applied to the Al target of the Rf sputtering system shown in Figure 1. This negative voltage attracts  $\text{Ar}^+$  ions to the target surface at a high speed. Generally, when a positive ion collides with atoms at the surface of a solid, an energy transfer occurs. If the energy transferred to a lattice site is greater than the binding energy, primary recoil atoms can be created, which can collide with other atoms and distribute their energy via collision cascades. A surface atom becomes sputtered if the energy transferred to the surface is larger than about heat of sublimation.

The polypropylene films were coated by condensation of Al metal atoms sputtered from the surface of Al target by high-energy  $\text{Ar}^+$  ions present in Ar plasma. Nucleation, growth of the Al crystals, and cohesion of crystals occur on the surface. The Al coating covers the holes and pores present at the surface and at the interface of zeolite particles and polypropylene. SEM showed that the surface of the films was coated with a smooth Al layer as shown in Figure 2(a,c). Films with and without zeolites had cracks on their surfaces nearly  $20\text{-}\mu\text{m}$  apart. The cracks formed in brittle Al surface during handling of the elastic polypropylene film Figure 2(b,d) show that the Al layer was composed of very small-sized particles having diameters around  $40\text{--}50$  nm. SEM microphotographs of cross sections of the films obtained by cutting by a scissor showed that there was a thin layer on the surface, which is different than the bulk of the film. A thin top layer of the poly(propylene) phase showed plastic deformation during cutting of the film, because it has an elongation at break value of  $164\%$ ,<sup>18</sup> and the brittle Al coating on the surface was broken into small pieces. This deformed thin layer of polypropylene with broken Al film on its surface was folded onto the cross section of the film. Thus, the Al coating could be examined in higher magnification. The Al layer having  $98$  and  $131$  nm thickness was brittle and broken into small fragments due to plastic deformation of poly(propylene) during cutting process as illustrated in Figure 3. This  $98$  and  $131\text{-nm}$  thick coating does not constitute a single layer; instead, the layer is formed by cohesion of small Al particles having around  $50$  nm size as seen in Figure 3(b,d).

EDX analysis was used to determine the elemental composition of the films. It was expected that pure poly(propylene) is composed of C and H elements, and coated poly(propylene) is composed of C, H, and Al elements. During processing of poly(propylene) films in air  $4\text{--}6$  wt %, oxygen was introduced to the surface of the films as seen in Table I. Presence of oxygen makes the interfacial adhesion of Al atoms to the surface.<sup>7</sup> All other samples had

TABLE I  
Weight % of Elements on the Surface of the Films by EDX Analysis

Wt % zeolite	Al-coating	C	O	Al	Na	Si	Cl	K	Ca	Fe
0	—	$93.05 \pm 4.29$	$6.95 \pm 4.29$	—	—	—	—	—	—	—
2	—	$69.75 \pm 2.16$	$13 \pm 4.53$	$1.87 \pm 0.11$	$10.28 \pm 0.17$	$2.92 \pm 1.51$	$0.96 \pm 0.13$	$0.14 \pm 0.07$	$2.39 \pm 1.74$	$8.69 \pm 2.52$
4	—	$90.31 \pm 7.15$	$6.2 \pm 3.66$	$0.68 \pm 0.7$	$0.31 \pm 0.03$	$0.37 \pm 0.7$	0	$0.05 \pm 0.05$	$1.77 \pm 2.74$	$0.31 \pm 0.01$
6	—	$95.58 \pm 0.46$	$3 \pm 0.2$	$0.28 \pm 0.11$	$0.31 \pm 0.14$	$0.36 \pm 0.08$	$0.16 \pm 0.06$	$0.15 \pm 0.05$	$0.16 \pm 0.03$	0
0	+	$89.19 \pm 2.83$	$4.61 \pm 0.43$	$6.2 \pm 3.21$	—	—	—	—	—	—
2	+	$84.63 \pm 0.32$	$3.83 \pm 0.31$	$9.23 \pm 0.17$	$0.41 \pm 0.02$	$0.33 \pm 0.09$	$0.1 \pm 0.03$	$0.13 \pm 0.12$	$0.21 \pm 0.09$	$1.13 \pm 0.07$
4	+	$83.42 \pm 0.44$	$4.46 \pm 0.08$	$9.91 \pm 0.31$	$0.45 \pm 0.31$	$0.53 \pm 0.06$	$0.15 \pm 0.06$	$0.2 \pm 0.04$	$0.24 \pm 0.11$	$0.64 \pm 0.6$
6	+	$83.74 \pm 0.42$	$4.2 \pm 0.24$	$10.02 \pm 0.35$	$0.5 \pm 0.07$	$0.48 \pm 0.19$	$0.21 \pm 0.24$	$0.25 \pm 0.11$	$0.38 \pm 0.12$	$0.18 \pm 0.31$

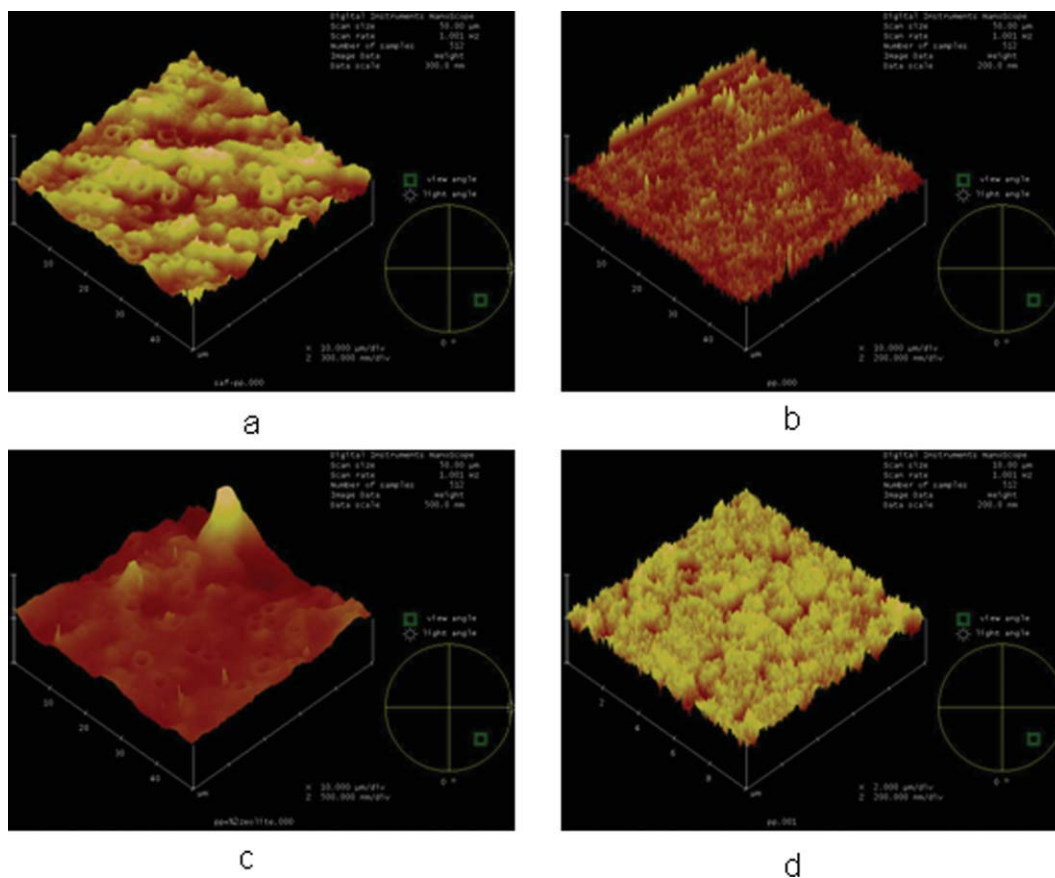


**Figure 4** Three-dimensional AFM micrographs of top of the films. (a) Control film, (b) Al-coated control film, (c) film with 2% zeolite, and (d) Al-coated film with 2% zeolite (the scale of the figures is 50  $\mu\text{m}$ ). [Color figure can be viewed in the online issue, which is available at [wileyonlinelibrary.com](http://wileyonlinelibrary.com).]

additionally Al, Na, Si, Cl, K, Ca, and Fe introduced by natural zeolites, which were mainly aluminosilicates. Al wt % values of Al-coated ones increased with respect to zeolite content from 6 to 10 wt % indicating zeolites created nucleation centers for Al crystal formation at the surface of the films. EDX analysis determined Al content at the surface as 6–10 wt % due to contribution of polymer layer beneath the Al coating to the analysis. This is a reasonable concentration, because the analytical depth of EDX is around 1–2  $\mu\text{m}$ .<sup>14</sup>

Figures 4 and 5 show AFM micrographs of uncoated and Al-coated films surfaces. Films without any zeolites also have solids added by the producer as seen in Figures 4(c) and 5(c) to prevent the slipping of the polymer film on rollers during film processing. These solid particles also act as nucleation centers for crystallization of polypropylene and increase the roughness of the film. Roughness data obtained from AFM are reported in Table II. The relationship between zeolite content and surface roughness is not very clear. Actually, it was expected to increase with increase in zeolite content. On the other hand, the reverse was observed in this study. The surface roughness of uncoted films decreased

from 9.49 to 4.37 nm as zeolite content increased from 0 to 6 wt %. The Al vapors seem to condense more on the tips of the peaks on the surface of the films, increasing surface roughness. Although the surface roughness of the uncoated films was in the range of 3.98–12.09 nm, the coated films had 8.45–16.46-nm surface roughness. Considering 50- $\mu\text{m}$  thickness of the films, the film surfaces were very smooth. Spherulitic structures around 5- $\mu\text{m}$  diameters and with wells at their centers are present on the surface of both uncoated and coated films. The cracks on the Al-coated films are also observed in AFM pictures.

Films had 30–42% crystallinity as measured by differential scanning calorimeter.<sup>17</sup> Figures 6 and 7 show X-ray diffraction diagrams of coated and uncoated samples. The polymer melt extruded from the die of the extruder was quenched by a chill roller and frozen to a solid and drawn by pull rollers. Thus, the film obtained had very small crystallites, because there was no time to grow. Thus, the crystalline peaks of polypropylene were broadened and overlapped due to presence of small crystallites. The Al-coated films also had similar broadened and overlapped peaks. The diffraction patterns in

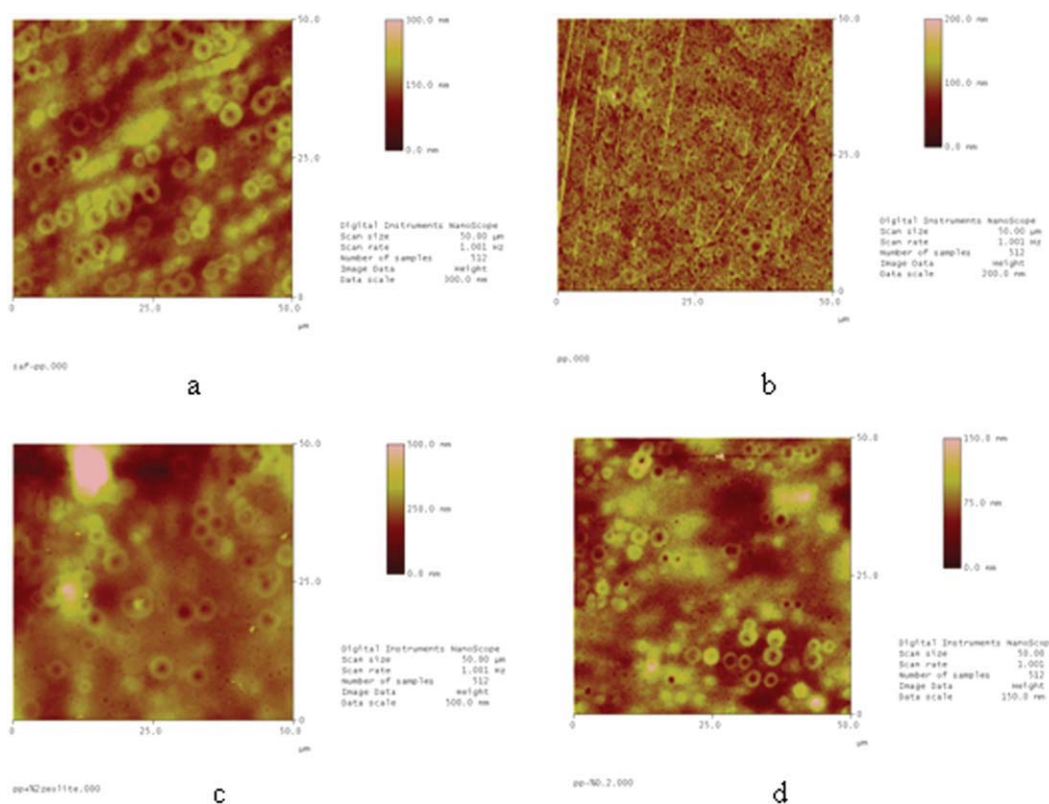


**Figure 5** AFM micrographs of top of the films. (a) Control film, (b) Al-coated control film, (c) film with 2% zeolite, and (d) Al-coated film with 2% zeolite (the scale of the figures is 50  $\mu\text{m}$ ). [Color figure can be viewed in the online issue, which is available at [wileyonlinelibrary.com](http://wileyonlinelibrary.com).]

Figures 6 and 7 are comprised predominantly of (110),(040), (130), (111), and (041) planes diffractions of isotactic  $\alpha$ -polypropylene. The diffractions of (110) and (040) planes at 14.6 and 17.2  $2\theta$  values reveal information about directions in which the  $a$  and  $b$  axes are oriented. If the ratio of intensities of (110) to (040) plane is less than 1.3, the  $b$  axis of polypropylene lies parallel to the film surface.<sup>20</sup> This ratio was determined as 1.3, 1.3, 1.2, and 1.1 for uncoated films having 0, 2, 4, and 6 wt % zeolite, respectively. This showed that  $b$ -axis of the poly(propylene) crystals was oriented parallel to the surface of the uncoated films.

(111) diffraction peak of Al metal was found as a very small peak around  $2\theta$  value of  $38^\circ$  in X-ray diagrams of coated films. From the breadth of this peak, grain size,  $B$  was calculated from Scherer's formula in eq. (1) and is shown in Table II.

$$B = 0.9 \times 0.1546/L \cos \theta \quad (1)$$

where  $L$  is breadth of the peak at half height in radians and  $\theta$  is peak maximum. Al grain sizes were found to be in the range of 22–29 nm as shown in Table II.

**TABLE II**  
Grain Size of Al, Surface Roughness, Light Absorbance at 250 and 600 nm, and Permeability of Water Vapor Through Films

Wt % zeolite	Al-coating	Grain size of Al (nm)	Roughness (nm)	Absorbance at 250-nm UV light	Absorbance at 600-nm visible light	Permeability $\times 10^5$ (( $\text{cm}^3/\text{s}$ )/( $\text{cm}^2 \text{ cm Hg}$ )) (cm)
0	Uncoated	–	12.09	0.16	0.06	0.75
2	Uncoated	–	8.77	0.56	0.33	1.45
4	Uncoated	–	3.98	0.60	0.32	1.5
6	Uncoated	–	5.94	0.46	0.27	1.5
0	Coated	–	16.46	0.39	0.30	0.70
2	Coated	29	8.45	1.66	1.18	0.88
4	Coated	23	12.45	2.66	2.31	0.99
6	Coated	23	10.01	2.66	2.34	0.88

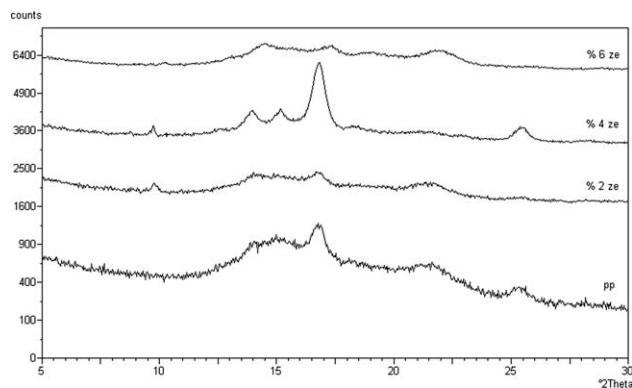


Figure 6 X-ray diffraction diagrams of uncoated films.

As reported in Table II while the films without Al coating were transparent to ultraviolet and visible light, Al-coated films had very high-absorbance values and did not transmit light in both regions of light spectrum. Although absorbance values for uncoated films were in the range of 0.06–0.33, the Al-coated films absorbance values were in the range of 0.39–2.66. The zeolite addition to poly(propylene) also increased the absorbance values but not sufficient enough to prevent light passing through. On the other hand, coating zeolite containing films with Al prevents light passing through the films. Coating of Al to the surface of zeolite-poly(propylene) composites lowered light transmission through the films in the same efficiency of Al-coated PET films<sup>12</sup> and PP films.<sup>14</sup>

Zeolites in the films had two different functions. They make the films porous and water vapor diffused from porous structure was adsorbed by the zeolite particles.<sup>18</sup> If one side of the films was coated by a thin Al layer filling pores between zeolite particles and poly(propylene), from this side, no water vapor will permeate through the films as represented in Figure 8. The water vapor permeability of the coated films was much lower than that of

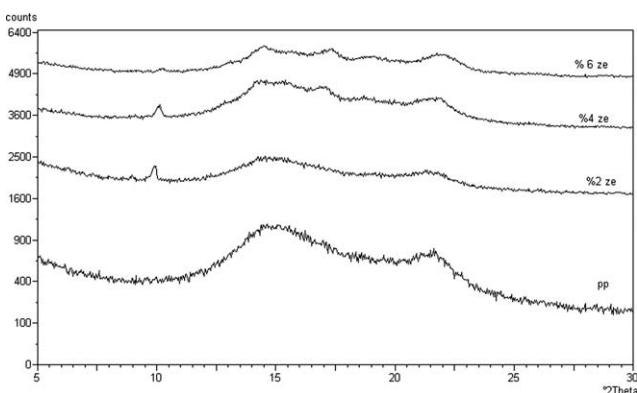


Figure 7 X-ray diffraction diagrams of Al coated films.

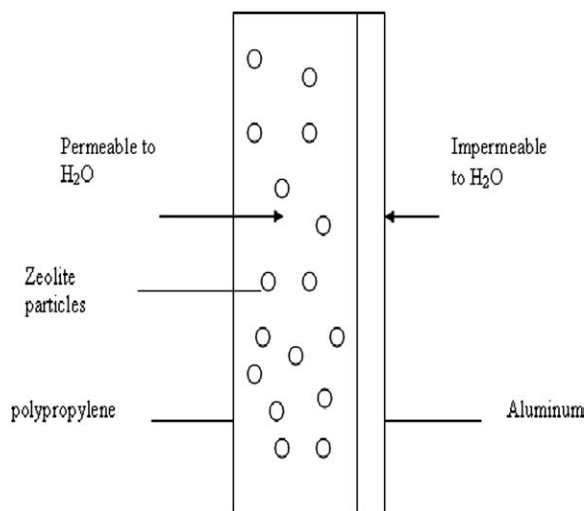


Figure 8 Packaging material impermeable to moisture from outside, but permeable from inside.

uncoated samples as reported in Table II. The permeability of film without zeolite slightly decreased by Al coating. It was 0.75 and  $0.70 \times 10^{-5}$  ((cm<sup>3</sup>/s)/(cm<sup>2</sup> cm Hg)) cm for uncoated and coated films. On the other hand, the films with zeolites had higher permeability values in the range of 1.45–1.50 ((cm<sup>3</sup>/s)/(cm<sup>2</sup> cm Hg)) cm. Their permeabilities decreased to 0.88–0.99 ((cm<sup>3</sup>/s)/(cm<sup>2</sup> cm Hg)) cm. Coating films with Al slowed down permeation of water vapor from the films but did not entirely prevent it. The cracks formed during handling of the coated films could be the reason of inefficient improvement in water vapor barrier properties.<sup>14</sup> Residual strain of coated films upon release of tensile stress may be the reason of this behavior.<sup>15,16</sup> Thus, lamination over Al layer by a polymer film, which does not permeate water vapor, could be a solution to this problem.

CONCLUSIONS

In this study, poly(propylene) zeolite composite films were coated with Al, and contribution of Al coating on film properties was investigated. Magnetron sputtering method was used for coating of poly(propylene) films with Al. Samples were characterized by EDX, X-ray diffraction, SEM, AFM, UV-vis spectroscopy, and water vapor permeation analyses. The surface was coated with pure Al layer of 98–131 nm thickness consisting of 50 nm particles with 22–29-nm grain sizes. Al percentage on the surface was determined to be 6–10 wt % as indicated with EDX analysis, due to contribution of polymer layer under Al surface. The surface roughness of the films increased during coating process. Permeation analysis showed that water vapor permeation rate

was lower for Al-coated materials. The coated films did not transmit light both in UV and visible region. The Al-coated films could be used as a packaging material, which prevents ingredients from the effects of undesired effects of UV and visible lights as well as moisture.

The authors thank for the support of State Planning Organization project number 2002K 120390.

## References

1. Shahidi, S.; Ghoranneviss, M.; Moazzenchi, B.; Anvari, E.; Rashidi, A. *Surf Coat Technol* 2007, 201, 5646.
2. Takano, I.; Inoue, N.; Matsui, K.; Kokubu, S.; Sasase, M.; Isobe, S. *Surf Coat Technol* 1994, 66, 509.
3. O'Hare, L. A.; Leadley, S.; Parbhoo, B. *Surf Interf Anal* 2002, 33, 335.
4. Moosheimer, U.; Bichler, C. H. *Surf Coat Technol* 1999, 116, 812.
5. Bichler, C. H.; Kerbstadt, T.; Langowski, H. C.; Moosheimer, U. *Surf Coat Technol* 1999, 112, 373.
6. Bichler, C. H.; Langowski, H. C.; Moosheimer U.; Seifert, B. *J Adhes Sci Technol* 1997, 11, 233.
7. Kurdi, J.; Ardelean, H.; Marcus, P.; Jonnard, P.; Arefi-Khonsari, F. *Appl Surf Sci* 2002, 189, 119.
8. Ueda, M.; Tan, I. H.; Dallaqua, R. S.; Rossi, J. O.; Barroso, J. J. *Tabacniks Nucl Inst Meth Phy Res B* 2003, 206, 760.
9. Pua, C. K.; Sheik, A. B. D.; Hamid, N.; Tan, C. P.; Mirhosseini, H.; Abd Rahman, R.; Rusul, G. *J Food Eng* 2008, 89, 419.
10. Seidel, C.; Kopf, H.; Gotsmann, B.; Vieth, T.; Fuchs, H.; Reihs, K. *Appl Surf Sci* 1999, 150, 19.
11. Taguchi, A.; Kitami, T.; Yamamoto, H.; Akamaru, S.; Hara, M.; Abe, T. *J Alloys Compounds* 2007, 441, 162.
12. Prosycevas, I.; Tamulevicius, S.; Guobiene, A.; Cyziute, C.; Ilnas, A.; Andrulovicus, M. *Superlattices Microstruct* 2004, 36, 79.
13. Fukuda, S.; Kawamoto, S.; Gotoh, Y. *J Thin Solid Films* 2003, 442, 117.
14. Rahmatollahpur, R.; Tahidi, T.; Jamshidi-Chaleh, K. *J Mater Sci* 2010, 45, 1937.
15. Yanaka, M.; Henry, B. M.; Roberts, A. P.; Grovenor, C. R. M.; Briggs, G. A. D.; Sutton, A. P.; Miyamoto, T.; Tsukahara, Y.; Takeda, N.; Chjater, R. *J Thin Solid Films* 2001, 397, 176.
16. Acharya, N. K.; Kulshrestha, V.; Awasthi, K.; Kumar, R.; Jain, A. K.; Singh, M.; Avasthi, D. K.; Vijay, Y. K. *Vacuum* 2006, 81389.
17. Tsubone, D.; Kodama, H.; Hasebe, T.; Hotta, A. *Surf Coat Technol* 2007, 21, 6431.
18. Özmihci, F.; Balköse, D.; Ülkü, S. *J Appl Polym Sci* 2001, 82, 2913.
19. Topcuoglu, O.; Altinkaya, S. A.; Balkose, D. *Prog Org Coat* 2006, 56, 269.
20. Cook, M.; Harper, J. F. *Adv Polym Technol* 2006, 17, 53.